

# Flow similitude laws applied to wind turbines through blade element momentum theory numerical codes

S. Brusca · R. Lanzafame · M. Messina

Received: 14 April 2014 / Accepted: 15 May 2014 / Published online: 2 August 2014  
© The Author(s) 2014. This article is published with open access at Springerlink.com

**Abstract** This paper deals with the analysis of the performance of different wind turbines using the Similitude Theory. Wind turbine performance was determined as a function of geometrical similarity coefficient, which is related to all parameters of the Similitude Theory. Therefore, a mathematical model simplification is possible in the ‘in similitude’ wind turbines comparison. The mathematical model for wind turbine performance is based on BEM Theory, and its efficacy was verified several times by comparing different wind turbine experimental data. The original mathematical model was modified to take into account Similitude Theory parameters. The model is able to determine which wind turbine is most suited to particular design specification. This work presents power and torque curves, power and torque coefficients as functions of rotational speed and wind velocity. All the results are function of the geometrical similarity coefficient. With this methodology it is possible to maximize the power coefficients of a wind turbine, and it is possible to identify a family of wind turbines, geometrically different, but with the same high performances.

**Keywords** BEM theory · Horizontal axis wind turbine · Flow similitude

## List of symbols

$R$	Rotor radius [m]
$\vartheta$	Twist angle [°]
$\alpha$	Angle of attack [°]
$D$	Rotor diameter [m]
$\phi$	Incoming flow direction angle [°]
$\omega$	Angular velocity [ $s^{-1}$ ]
$a$	Axial induction factor [–]
$a'$	Tangential induction factor [–]
$r$	Blade local radius [m]
$V_0$	Wind velocity far up stream [m/s]
$N$	Rotor normal force [N]
$(V_0)_{\text{effective}}$	Wind axial velocity immediately before the rotor [m/s]
$U$	Absolute blade tangential velocity [m/s]
$U_{\text{effective}}$	Tangential component of wind velocity relative to the blade [m/s]
$h_g$	Geometrical similarity coefficient [–]
$h_c$	Kinematic similarity coefficient [–]
$n$	Rotational velocity [r/min]
$c_q$	Torque coefficient [–]
$N_b$	Number of blades [–]
$\rho$	Air density [ $kg/m^3$ ]
$Ma$	Mach number [–]
$\mu$	Kinematic viscosity [Pa s]
$F$	Prandtl tip loss factor [–]
$C_N$	Normal force coefficient [–]
$\lambda$	Tip speed ratio [–]
$\lambda_r$	Local tip speed ratio [–]
$c$	Airfoil chord [m]
$C_L$	Airfoil lift coefficient [–]
$C_D$	Airfoil drag coefficient [–]
$c_p$	Power coefficient [–]
$T$	Torque [Nm]
$P$	Power [W]

S. Brusca  
Department of Chemical, Electronic and Industrial Engineering,  
University of Messina, Messina, Italy

R. Lanzafame · M. Messina (✉)  
Department of Industrial Engineering, University of Catania,  
Catania, Italy  
e-mail: mmessina@dii.unict.it

$V_1$	Airfoil relative wind velocity [m/s]
$Re$	Reynolds number [–]
$\sigma$	Rotor solidity [–]
$I$	Turbulence intensity [–]

### Abbreviations

BEM	Blade element momentum
AEP	Annual energy production
DOE/NREL	US Department Of Energy/National Renewable Energy Laboratory
1-D	One-dimensional
2-D	Two-dimensional
3-D	Three-dimensional
CSU	Colorado State University
OSU	Ohio State University
DUT	Delft University of Technology

### Subscript

A	Wind turbine “A”
B	Wind turbine “B”

### Introduction

Wind turbine performance evaluation is important in optimal wind turbine design for specific installation sites. Therefore, the performances of many turbines should be evaluated to make the best choice. Accordingly, a fast and reliable design tool is crucial for quickly evaluating different wind turbine performances. Nowadays, this tool is a mathematical model based on Blade Element Momentum Theory (BEM Theory). These tools are implemented as 1D codes and they are extremely fast in terms of computer running times. Mathematical models based on BEM Theory are mono-dimensional (1D) codes making them very fast but losing some precision. Thus, the best trade-off between precision and running time must be found.

Nowadays, a lot of university and industrial researchers are working on making BEM codes more precise, and optimizing mathematical models and their implementation [1–11]. Consequently, computer codes based on BEM Theory are becoming so fast and precise that they are commonly used in universities and industry as design tools and wind turbine performance evaluators. These models are very powerful for studying wind turbine performance as a function of turbine geometry in a very short time.

However, some critical BEM Theory implementation issues [12–24] should also be faced up to and solved. These critical issues cause numerical instabilities that yield non-convergent codes. Various authors have treated these critical issues in different ways obtaining different solutions. The best solution is high code precision. The critical issues

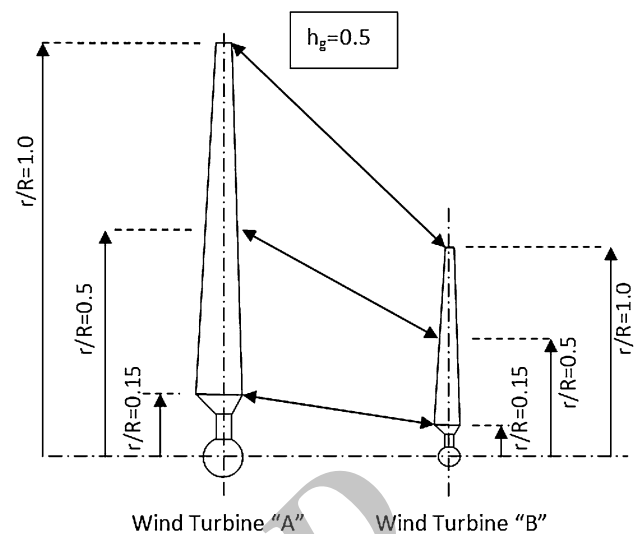


**Fig. 1** Homologous sections of two wind turbines in a fluid dynamic similarity condition

relate to the correct mathematical representation of the tangential and axial induction coefficients [25] of the 2D aerofoil lift and drag coefficients [26, 27] as well as the radial fluxes along the turbine blades. The latter are 3D phenomena and it is difficult to account for them in a 1D model. This can be done using specific mathematical expedients [13].

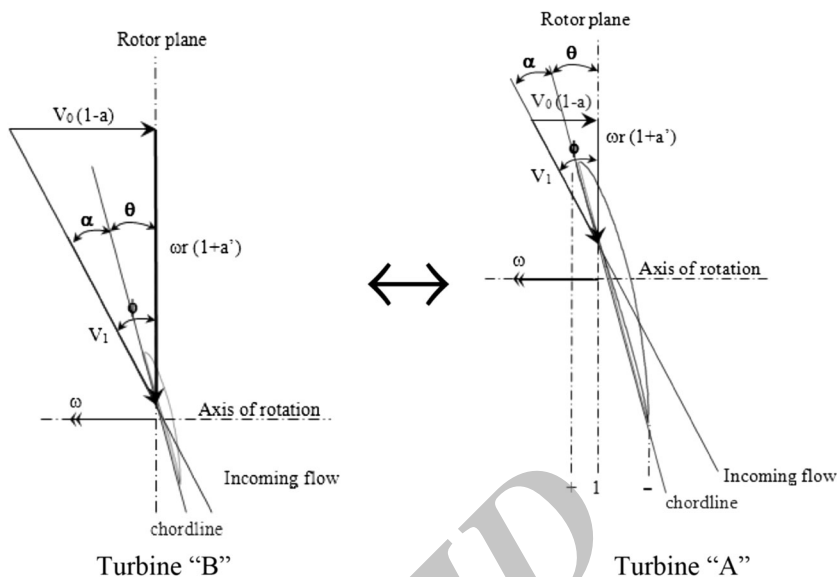
In this work, the authors modified an existing BEM Theory-based mathematical model [12] for wind turbine performance evaluation, adapting it to parametric dimensional analyses. The advantage of this relates to being able to evaluate wind turbine performance in fluid dynamic similarity conditions.

### Flow similitude laws applied to wind turbines

Using the Buckingham Theorem [28, 29] wind turbine performance can be made analogous through the results obtained for other wind turbines by imposing similitude conditions. The scientific literature makes two distinctions: (a) determining wind turbine (under study) performance using the performance data of a scaled-down turbine (model) obtained experimentally, (b) studying wind turbine performance as a function of environmental conditions.

To validate an ‘in similitude’ study, geometrical, kinematic and dynamic similarity must be verified at the same time. This occurs when non-dimensional wind turbine numbers are shared by two turbines. These numbers are: rotor solidity  $\sigma$ , Reynolds number  $Re$ , Tip Speed Ratio  $\lambda$ , Mach number  $Ma$ , lift coefficient  $C_L$ , drag coefficient  $C_D$  and ambient turbulence intensity  $I$ .

**Fig. 2** Velocity triangles in homologous sections ( $r/R$ )<sub>B</sub> = ( $r/R$ )<sub>A</sub>: kinematic similarity



**Geometrical similarity**

To have two geometrically similar wind turbines, the dimensional ratio of homologous sections (see Fig. 1) should be constant as in Eq. (1).

$$D_B/D_A = h_g \tag{1}$$

The ratio between homologous sections must be equal to  $h_g$ . Thus, the ratio between every geometric dimension of turbine B (model) and the homologous geometric dimension of turbine A (under study) must be equal to  $h_g$ . The parameter  $h_g$  is called the geometric similarity coefficient.

Naturally, geometrical similarity requires that wind turbines in similitude conditions have the same number of blades. This can be obtained using the equality of rotor solidity [see Eqs. (2), (3)].

$$\sigma_B = \sigma_A \tag{2}$$

$$\frac{(N_b)_B C_B}{\pi R_B} = \frac{(N_b)_A C_A}{\pi R_A} \tag{3}$$

Eq. (3) leads to Eq. (4)

$$(N_b)_B = (N_b)_A \cdot \frac{c_A}{c_B} \cdot \frac{R_B}{R_A} \tag{4}$$

Considering that the ratio between homologous geometric dimensions is equal to the geometrical similarity coefficient, then Eq. (5) is:

$$\frac{C_A}{C_B} = \frac{R_A}{R_B} = \frac{1}{h_g} \tag{5}$$

This leads to Eq. (6):

$$(N_b)_B = (N_b)_A \tag{6}$$

Therefore, the blade number of turbine “A” must be the same for turbine “B”.

**Kinematic similarity**

To have kinematic similarity, the velocity triangles in homologous sections should be geometrically similar (Fig. 2). All homologous velocities must be scaled down with the same kinematic similarity coefficient  $h_c$  [see Eq. (7)].

$$h_c = \frac{(V_0)_B}{(V_0)_A} \tag{7}$$

Equating the Reynolds Numbers [Eq. (8)]

$$Re_B = Re_A \tag{8}$$

this leads to Eq. (9)

$$\frac{\rho_B (V_0)_B c_B}{\mu_B} = \frac{\rho_A (V_0)_A c_A}{\mu_A} \tag{9}$$

Using Eq. (9), the kinematic similarity coefficient can be obtained as in Eq. (10).

$$\frac{(V_0)_B}{(V_0)_A} = \left(\frac{\rho_A}{\rho_B}\right) \cdot \left(\frac{\mu_B}{\mu_A}\right) \cdot \left(\frac{c_A}{c_B}\right) = h_c \tag{10}$$

Using the same fluid at the same temperature and pressure, the density and dynamic viscosity ratios equal 1 [see Eq. (11)].

$$\left(\frac{\rho_A}{\rho_B}\right) = \left(\frac{\mu_B}{\mu_A}\right) = 1 \tag{11}$$

Combining Eqs. (5) and (11) leads to Eq. (12):

$$\frac{(V_0)_B}{(V_0)_A} = \left(\frac{c_A}{c_B}\right) = \frac{1}{h_g} \quad (12)$$

Thus, equating Eqs. (10) and (12), the link between the kinematic and geometrical similarity coefficients (13) is obtained:

$$h_c = \frac{1}{h_g} \quad (13)$$

By applying the kinematic similarity law and equating the two tip speed ratio (TSR) it is possible to obtain Eq. (14):

$$\frac{\omega_B R_B}{(V_0)_B} = \frac{\omega_A R_A}{(V_0)_A} \quad (14)$$

Eq. (14), leads to Eq. (15):

$$\omega_B = \omega_A \cdot \frac{R_A}{R_B} \cdot \frac{(V_0)_B}{(V_0)_A} = \omega_A \cdot \frac{1}{h_g} \cdot h_c = \frac{\omega_A}{(h_g)^2} \quad (15)$$

and consequently Eq. (16):

$$n_B = \frac{n_A}{(h_g)^2} \quad (16)$$

In Fig. 2,  $a$  and  $a'$  are the axial and tangential induction factors, respectively [12]. Taking into account the definition of  $a$  and  $a'$ , Eqs. (17) and (18) are:

$$a = \frac{\Delta V_0}{V_0} = \frac{V_0 - (V_0)_{\text{effective}}}{V_0} \quad (17)$$

where  $V_0$  is the undisturbed upstream wind turbine axial velocity, and  $(V_0)_{\text{effective}}$  is the axial velocity just upstream of the rotor.

$$a' = \frac{\Delta U}{U} = \frac{U_{\text{effective}} - U}{U} \quad (18)$$

where  $U_{\text{effective}}$  is the tangential velocity relative to the airfoil, and  $U$  is the tangential velocity of the blade.

Equation (7) is valid for each homologous velocity. Thus, it is demonstrable that:

$$a_A = a_B \quad (19)$$

$$a'_A = a'_B \quad (20)$$

From Fig. 2, it is possible to notice that [see Eq. (21)]:

$$\phi = \arctan \frac{V_0(1-a)}{\omega r(1+a')} \quad (21)$$

For turbine “B”:

$$\phi_B = \arctan \frac{(V_0)_B(1-a_B)}{\omega_B r_B(1+a'_B)} \quad (22)$$

Taking into account Eqs. (1), (7), (13), (15) and (19), (23) is:

$$\phi_B = \arctan \frac{(1/h_g)(V_0)_A(1-a_A)}{\frac{\omega_A}{h_g} h_g r_A (1+a'_A)} = \phi_A \quad (23)$$

Dynamic similarity

To have dynamic similarity, the lift  $C_L$  and drag  $C_D$  coefficients should be equal in homologous sections. For the homologous sections of any specific airfoil, the drag and lift coefficients are a function of the Reynolds number and angle of attack (see Figs. 3, 4).

Therefore, to have equal drag and lift coefficients in homologous sections, the Reynolds numbers (Eq. 8) as well as the angles of attack must be equal.

$$\alpha_A = \alpha_B \quad (24)$$

From Fig. 2, it can be deduced that:

$$\phi = \alpha + \theta \quad (25)$$

and taking into account Eqs. (23), (24) and (25), it is necessary to have:

$$\theta_A = \theta_B \quad (26)$$

In conclusion, to have two wind turbines (with the same fluid, temperature and pressure) ‘in flow similitude’, homologous sections must have the same airfoil and the same twist [see Eq. (26)].

Blade element momentum theory

The numerical code developed is a 1D code for the design of Horizontal Axis Wind Turbines. It has very fast processing times (less than one second) and is highly accurate in numerical simulations. This code is based on Blade Element Momentum (BEM) Theory, and can be applied to wind rotor design, and/or evaluating its performance. It is a useful tool for research and industry in wind turbine design. This numerical code can maximize wind rotor power, control the power curve, maximize Annual Energy Production (AEP), and help develop innovative layouts for wind turbines [1, 25, 26].

The code has been refined in recent years by comparing wind rotor experimental data obtained in wind tunnels [30] or through field testing [31]. In the past, comparisons were carried out by two different wind rotors using the same airfoil [13].

BEM Theory-based numerical codes subdivide the wind turbine rotor into annuli of  $dr$  thickness [12], the flow of each sector being independent of adjacent circular sector flows [32]. By applying the equations of momentum and angular momentum conservation, for each infinitesimal  $dr$  sector of the blade, axial force and torque can be defined [Eqs. (27), (28)].

**Fig. 3** S809 airfoil lift coefficient

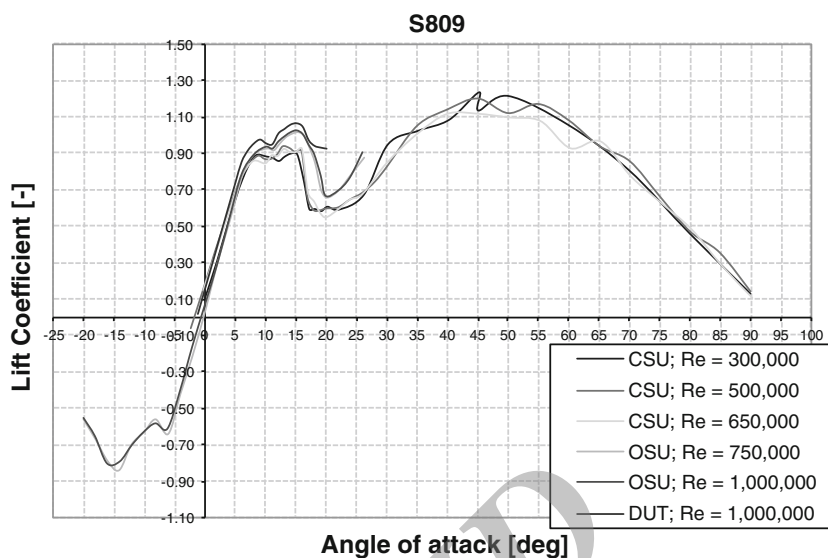
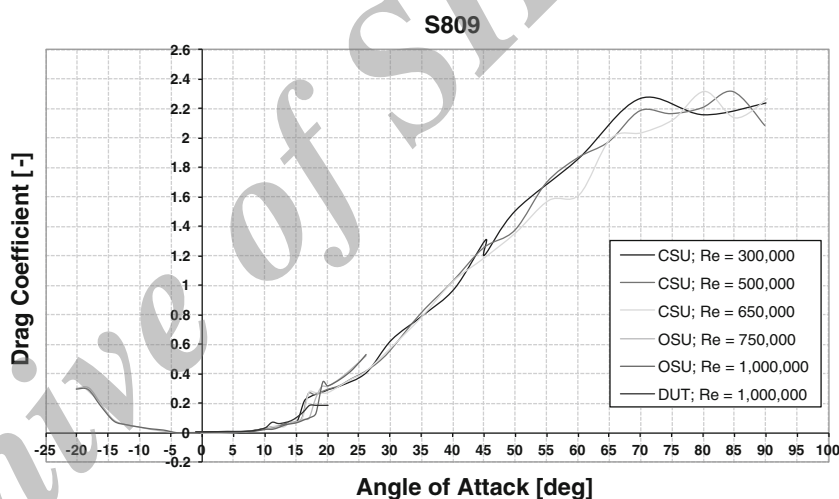


**Fig. 4** S809 airfoil drag coefficient



The axial force on the blade element of width  $dr$  is:

$$dN = \frac{\rho V_0^2 (1-a)^2}{2 \sin^2 \phi} N_b (C_L \cos \phi + C_D \sin \phi) c dr \quad (27)$$

The torque on the blade element of width  $dr$  is:

$$dT = \frac{\rho V_0 (1-a)}{2 \sin \phi} \cdot \frac{\omega r (1+a')}{\cos \phi} N_b (C_L \sin \phi - C_D \cos \phi) c r dr \quad (28)$$

Knowing the lift and drag coefficients ( $C_L$  and  $C_D$ ) is of crucial importance in assessing the forces and torques according to Eqs. (27) and (28).

Obviously, the geometry of the wind rotor is the input within the numerical code for evaluating rotor performance.

The numerical stability of the mathematical code depends on tangential and axial induction factors.

Equations (29), (30) and (31) report the induction factors implemented inside the numerical code [12]:

For  $a < 0.4$ :

$$a = \frac{1}{\frac{4F \sin^2 \phi}{\frac{c N_b}{2\pi r_1} (C_L \cos \phi + C_D \sin \phi)} + 1} \quad (29)$$

while for  $a \geq 0.4$  [33]:

$$a = \frac{18F - 20 - 3\sqrt{C_N(50 - 36F) + 12F(3F - 4)}}{36F - 50} \quad (30)$$

and

$$a' = \frac{1}{2} \left( \sqrt{1 + \frac{4}{\lambda_r^2} a(1-a)} - 1 \right) \quad (31)$$

where  $F$  is the Prandtl Tip Loss Factor, as reported in [18, 20].

The mathematical code proposed in this work has been validated in [13, 34] through a comparison with experimental data found in scientific literature. The comparison has been done for two different wind turbines, evidencing a very little error between numerical data and experimental data. The two turbines were: the NREL Phase II [32], a wind turbine with three blades, 10.6 m rotor diameter, with un-tapered and un-twisted blades, developing a rated power of 19.8 kW and the NREL Phase VI turbine [31], a wind turbine with two blades, 10.6 m diameter, with tapered and twisted blades, developing 10 kW of rated power.

**Performance characteristics**

With wind turbine A (Phase VI) as the reference turbine (characteristic curves are known experimentally [18] and numerically [12]), varying the geometrical similarity coefficient  $h_g$  produces various characteristic curves of the turbines running ‘in flow similitude’ condition. The mathematical model can be verified by comparing the non-dimensional groups for each turbine. This means that  $c_p - \lambda$  and  $c_q - \lambda$  must be independent of the specific geometrical similarity coefficient.

Figure 5 shows three different wind turbines ‘in similitude’ with different geometrical similarity coefficients ( $h_g = 0.4, 1.0$ , and  $3.0$ ). The turbine with the geometrical similarity coefficient of  $1.0$  is the above-mentioned reference turbine (Phase VI).

Increasing the geometrical similarity coefficient, the wind turbine’s geometric dimensions increase and, at the same time, the wind velocity at which to evaluate turbine performance proportionally decreases.

Figure 6 shows the simulation results for  $h_g$  varying from  $0.4$  to  $3.0$ .

From Fig. 6, the power and torque coefficient trends overlap as the geometrical similarity coefficient varies. In particular, the power coefficient reaches its maximum value ( $c_p = 0.37$ ) at  $\lambda = 6.3$ , while the torque coefficient reaches its maximum value ( $c_q = 0.0655$ ) at  $\lambda = 4.8$ . In this work, the hypothesis of incompressible fluids is made ( $Ma$  number is less than  $0.3$  in all sections). In a wind turbine, the maximum velocity occurs at the blade tip. As geometrical similarity coefficients ( $V_B = V_A/h_g$ ) decrease, velocities increase. Thus, in an ‘in similitude’ study, the minimum possible value of geometrical similarity coefficient is  $h_g = 0.4$  and, consequently the  $Ma$  at the blade tip is  $0.28$ .

**Fig. 5** Three wind turbines in fluid dynamic similarity

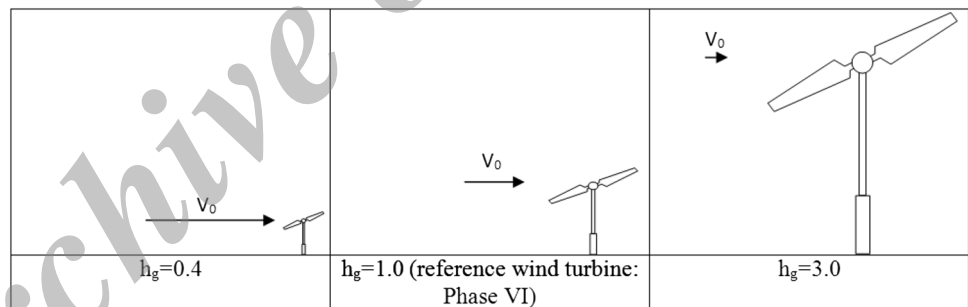


**Fig. 6** Similitude condition running characteristic wind turbine curves varying the geometrical similarity coefficient

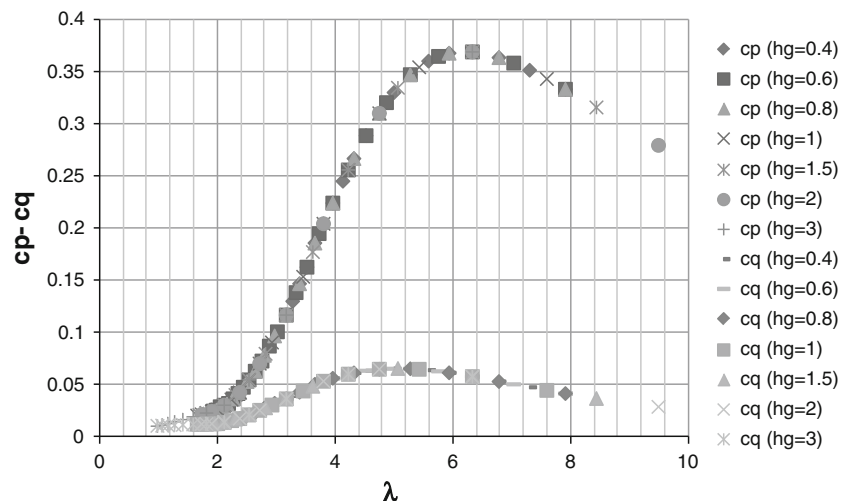


**Fig. 7** Power curves as a function of wind speed for three different geometrical similarity coefficients

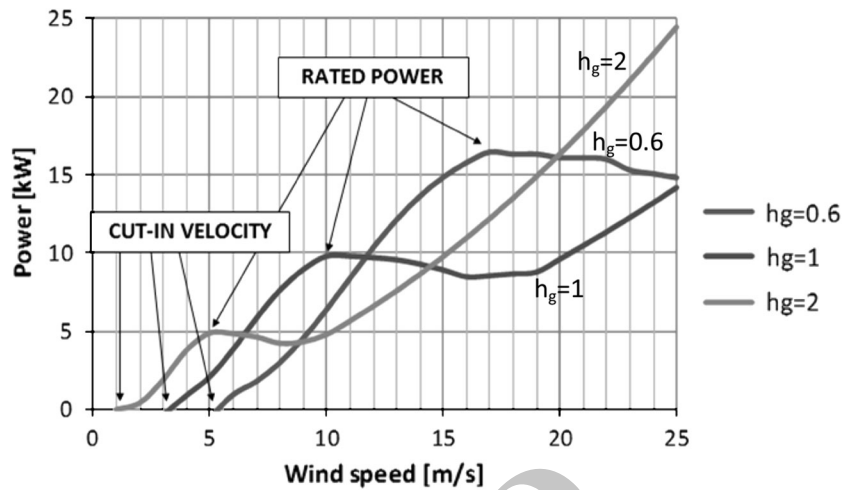


**Fig. 8** Torque curves as functions of wind speed for seven different geometrical similarity coefficients

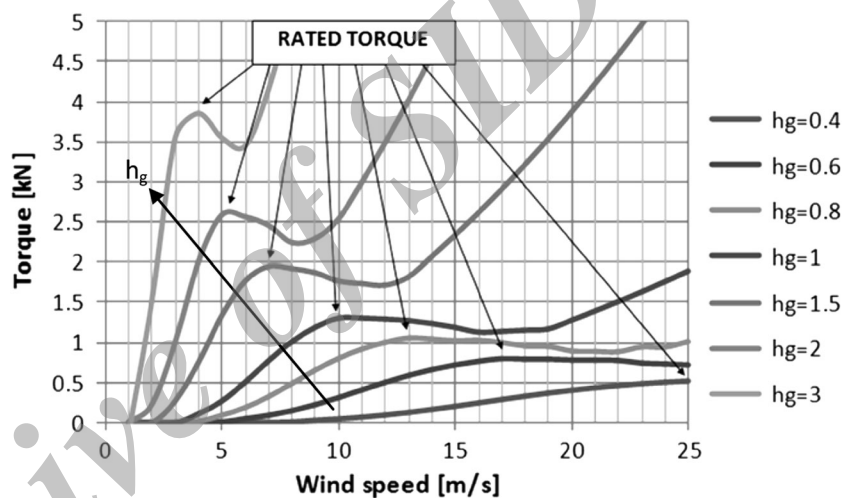
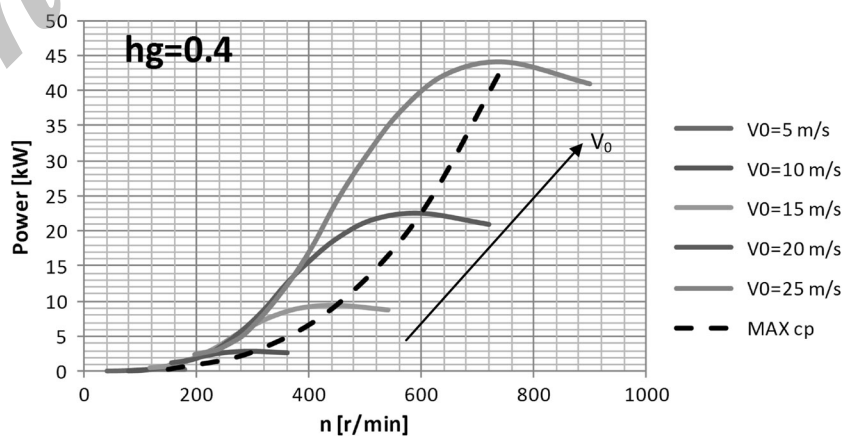


**Fig. 9** Power–rotational speed curve ( $h_g = 0.4$ )



Using a mathematical model based on BEM Theory, torque and power curves can be evaluated as functions of geometrical similarity coefficients.

Figure 7 shows the power curves for three different geometrical similarity coefficients as functions of wind

speeds. Notice in Fig. 7, that the three turbines have different cut-in velocities, as well as different design powers. These parameters are very important in choosing the wind turbine for a specific installation site. Figure 8 shows torque curves as functions of wind speeds. Notice in Fig. 8,

**Fig. 10** Torque–rotational speed curve ( $h_g = 0.4$ )

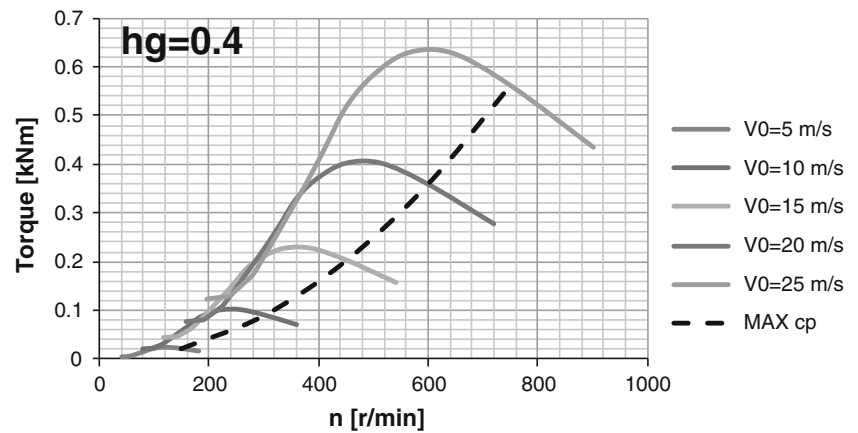


**Fig. 11** Power–rotational speed curve ( $h_g = 1.0$ )

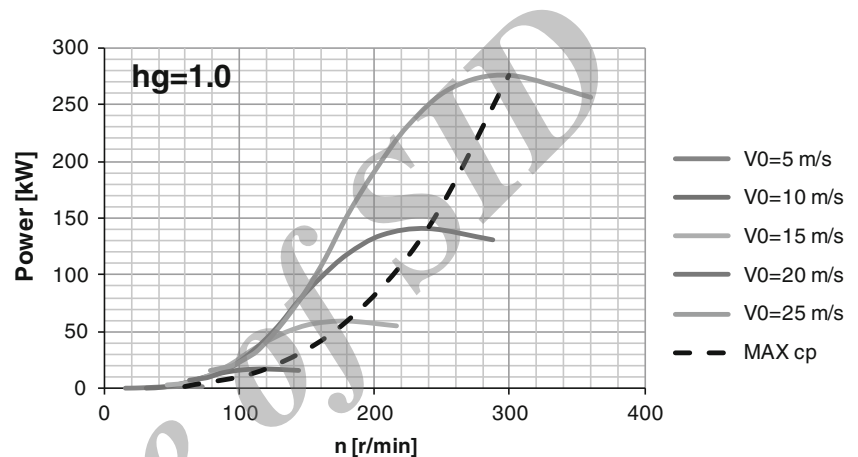
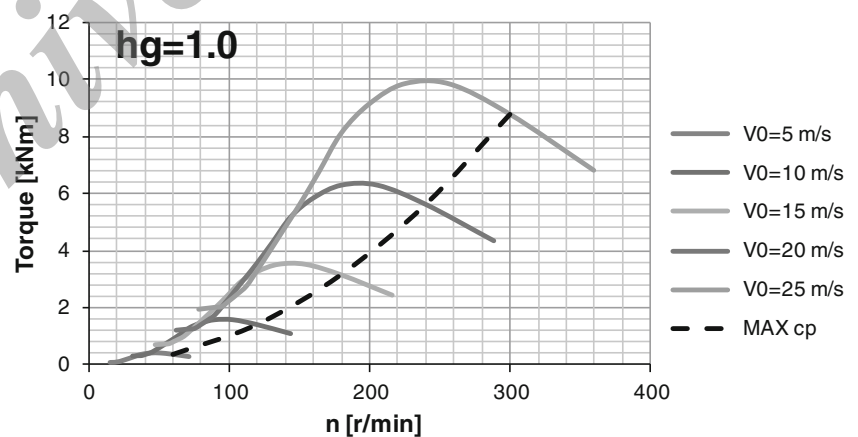


**Fig. 12** Torque–rotational speed curve ( $h_g = 1.0$ )



that each turbine has different design torques (for different wind speeds) varying according to geometrical similarity coefficients.

Figures 9, 10, 11, 12, 13, 14 show the specific turbine characteristic curves (power vs  $n$  and torque vs  $n$ ) for three geometrical similarity coefficients (0.4, 1.0 and 3.0).

The mathematical model is able to calculate power and torque curves as functions of turbine rotational speeds varying with geometrical similarity coefficient. These

characteristic curves are very useful for matching the electric generator.

Figures 10, 11 and 14 show torque vs rotational speed curves as functions of both wind speed and geometrical similarity coefficient. The “MAX  $c_p$ ” curve is also reported which is the set of maximum power coefficient values in the torque–rotational speed graph. For each graph, a value was obtained for when the power coefficient reaches its maximum value ( $c_p = 0.37$ ) at a tip speed ratio of 6.3



**Fig. 13** Power–rotational speed curve ( $h_g = 3.0$ )

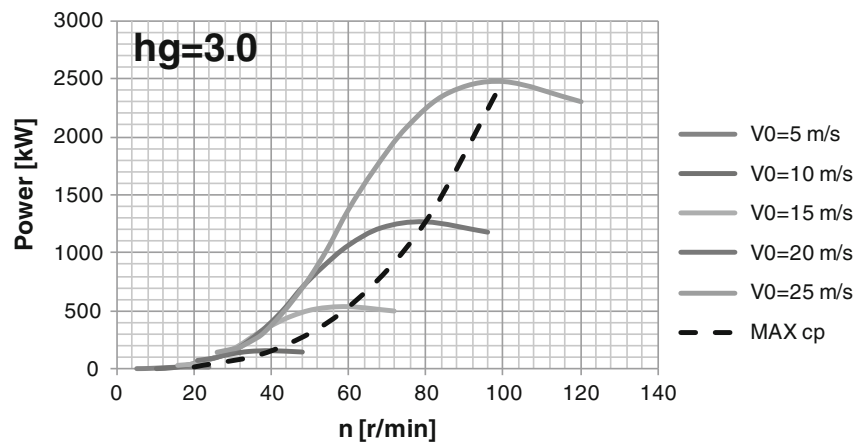
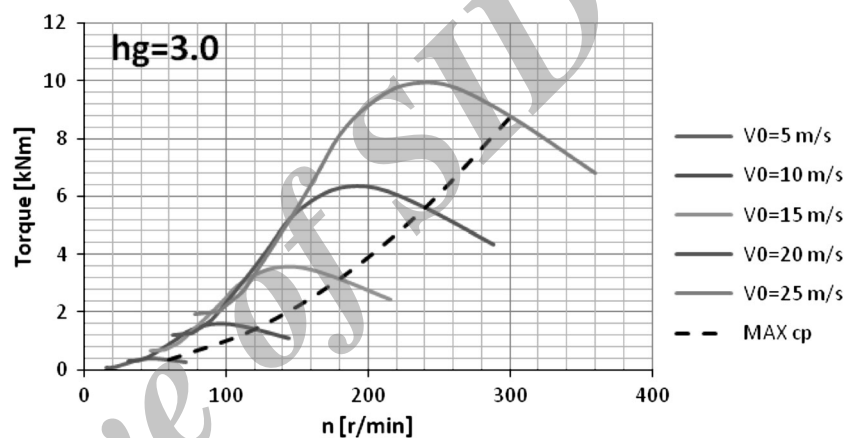


**Fig. 14** Torque–rotational speed curve ( $h_g = 3.0$ )



(see Fig. 6). Then, all these maximum values were plotted to create the MAX  $c_p$  curve.

These graphs can be used to match a suitable electric generator to each specific wind turbine, as well as in designing the relative turbine control systems.

## Conclusions

Using fluid dynamic similitude studies, the authors have developed and implemented a mathematical model for horizontal axis wind turbine design and performance evaluation. The model is based on the Momentum Conservation Law of rotor blade elements (BEM Theory). The first version of the mono-dimensional model, implemented and tested by the same authors over several years, can run a huge number of simulations in a very short time.

In this work, the code was modified to take into account fluid dynamic similitude in wind turbine design and performance evaluation. This code is a powerful tool for evaluating the characteristic curves of a many wind

turbines that are geometrically different, but in flow similitude conditions.

This is a novel approach of fluid dynamic similitude in wind turbine studies. It can evaluate the performance of a whole set of wind turbines very fast and identify the most suitable wind turbine for the site specifications.

The code can identify wind turbines with different cut-in velocities, torques and powers, as well as different mechanical characteristic curves. Fluid dynamic characteristic curves (torque and power as functions of wind speeds) are used to calculate annual energy production in specific sites, while mechanical characteristic curves are used to match the wind turbine with the optimal electric generator. Moreover, the reference wind turbine can be optimized to have a maximum power coefficient value and, taking into account similitude laws, can identify all the wind turbines with different geometrical dimensions, cut-in velocities, torques and powers, but with the same high value of the reference wind turbine's power coefficient.

**Open Access** This article is distributed under the terms of the Creative Commons Attribution License which permits any use,

distribution, and reproduction in any medium, provided the original author(s) and the source are credited.

## References

- Lanzafame, R., Messina, M.: Design and performance of a double-pitch wind turbine with non-twisted blades. *Renewable energy*. Elsevier Sci. **34**(5), 1413–1420 (2009)
- Pinheiro Vaz, J.R., Pinho, J.T., Amarante Mesquita, A.L.: An extension of BEM method applied to horizontal-axis wind turbine design. *Renewable energy*. Elsevier Sci. **36**, 1734–1740 (2001)
- McWilliam, M., Crawford, C.: The behavior of fixed point iteration and Newton-Raphson methods in solving the blade element momentum equations. *Wind Eng.* **35**(1), 17–32 (2011)
- Dai, J.C., Hub, Y.P., Liu, D.S., Long, X.: Aerodynamic loads calculation and analysis for large scale wind turbine based on combining BEM modified theory with dynamic stall model. *Renew. Energy* **36**, 1095–1104 (2011)
- Rajakumar, S., Ravindran, D.: Iterative approach for optimising coefficient of power, coefficient of lift and drag of wind turbine rotor. *Renew. Energy* **38**, 83–93 (2012)
- Nagai Baku, M., Ameku Kazumasa, Roy Jitendro Nath, : Performance of a 3 kW wind turbine generator with variable pitch control system. *Appl. Energy* **86**, 1774–1782 (2009)
- Kazumasa, Ameku, Nagai Baku, M., Roy Jitendro Nath, : Design of a 3 kW wind turbine generator with thin airfoil blades. *Exp. Thermal Fluid Sci.* **32**, 1723–1730 (2008)
- Choi, N.J., Nam, S.H., Kim, J.S., Lee, M.S., Kim, K.C.: CFD study on power output and flow characteristics of 110 kW class BAWT. Istanbul, Turkey. In: International conference on high performance computing and simulation (HPCS), IEEE Computer Society, Los Alamitos, CA, USA, p 859–64 2011
- Minami, Y., Nimura, T., Sasaki, N., Murayama, H., Uzawa, K., Wada, H.: “Development of tidal and ocean current power plant using elastic turbine”, underwater technology (UT). In: 2011 IEEE symposium and 2011 workshop on scientific use of submarine cables and related technologies (SSC), 1–6 (2011)
- Duan Wei, Zhao Feng.: Loading analysis and strength calculation of wind turbine blade based on blade element momentum theory and finite element method. In: Power and energy engineering conference (APPEEC), Asia-Pacific, 1–4 (2010)
- Tenguria Nitin, Mittal, N.D., Ahmed Siraj, : Investigation of blade performance of horizontal axis wind turbine based on blade element momentum theory (BEMT) using NACA airfoils. *Int. J. Eng. Sci. Technol.* **2**(12), 25–35 (2010)
- Lanzafame, R., Messina, M.: Fluid dynamics wind turbine design: critical analysis, optimization and application of BEM theory. *Renewable energy*. Elsevier Sci. **32**(14), 2291–2305 (2007)
- Lanzafame, R., Messina, M.: BEM theory: how to take into account the radial flow inside of a 1-D numerical code. *Renew. Energy* **39**, 440–446 (2012)
- Hansena, M.O.L., Sørensen, J.N., Voutsinas, S., Sørensen, N., Madsen, H.A.: State of the art in wind turbine aerodynamics and aeroelasticity. *Prog. Aerosp. Sci.* Elsevier Sci. **42**, 285–330 (2006)
- Johansen, J., Sørensen, N.N.: Aerofoil characteristics from 3D CFD rotor computations. *Wind Energy* **7**(4), 283–294 (2004)
- Snel, H., Houwink, B., Bosschers, J., Piers, W. J., Van Bussel, G. J. W., Bruining, A.: Sectional prediction of 3-D effects for stalled flow on rotating blades and comparison with measurements. In: Proceedings of the ECWEC 1993, Travemunde, 395–9 1993
- Chaviaropoulos, P.K., Hansen, M.O.L.: Investigating three-dimensional and rotational effects on wind turbine blades by means of a quasi-3D Navier-Stokes solver. *J. Fluids Eng.* **122**, 330–336 (2000)
- Bak, C., Johansen, J.: Three-dimensional corrections of airfoil characteristics for wind turbines based on pressure distributions. In: Proceedings of the EWEC conference 2006
- Lindenburt, C.: Investigation into rotor blade aerodynamics. ECN-C-03-025, (2003)
- Bermudez, L., Velazquez, A., Matesanz, A.: Viscous–inviscid method for the simulation of turbulent unsteady wind turbine airfoil flow. *J. Wind Eng. Ind. Aerodyn.* **90**, 643–661 (2002)
- Corten, G.P.: Flow separation on wind turbine blades. PhD. thesis, Utrecht University (2001)
- Sphera, D.A. (ed.): Wind turbine technology: fundamental concepts of wind turbine engineering. American Society of Mechanical Engineers, Fairfield (2009)
- Himmelskamp, H.: 1950. Profiluntersuchungen an Einem Umlaufenden Propeller, Diss. Goettingen, Max-Planck-Inst. fuer Stroemungsforschung, Goettingen, Report No. 2 (1945)
- Battisti, L.: Gli impianti motori eolici. Green Place Energies (2011)
- Maalawi, K.Y., Negm, H.N.: Optimal frequency design of wind turbine blades. *J. Wind Eng. Ind. Aerodyn.* **90**, 961–986 (2002)
- Lanzafame, R., Messina, M.: Optimal wind turbine design to maximize energy production. *Proc. IMechE*, part A. *J. Power Energy* **223**, 93–101 (2009)
- Lanzafame, R., Messina, M.: Power curve control in micro wind turbine design, energy. Elsevier Sci. **35**(2), 556–561 (2010)
- Lanzafame, R., Messina, M.: Horizontal axis wind turbine working at maximum power coefficient continuously. *Renew. Energy* **35**, 301–306 (2010)
- Buhl, L. Jr.: A new empirical relationship between thrust coefficient and induction factor for the turbulent windmill state. Technical Report NREL/TP-500-36834 (2005)
- Buckingham, E.: On physically similar systems; illustrations of the use of dimensional analysis. *Phys. Rev.* **4**, 345–376 (1914)
- Jonkman, J.M.: Modeling of the UAE wind turbine for refinement of FAST\_AD. NREL/TP-500-34755, (2003)
- Schepers, J.G., Brand, A.J., Bruining, A., Graham, J.M.R., Hand, M.M., Infield, D.G. et al.: “Final report of IEA Annex XIV : field rotor aerodynamics”, ECN (Energy research Centre of the Netherlands) Report—ECN-C-97-027 (1997)
- Moriarty, P.J., Hansen, A.C.: “AeroDyn theory manual”, Technical Report NREL/TP-500-36881 (2005)
- Lanzafame, R., Messina, M.: Advanced brake state model and aerodynamic post-stall model for horizontal axis wind turbines. *Renew. Energy* **50**, 415–420 (2013)

